Extended Abstracts of the 20th (1988 International) Conference on Solid State Devices and Materials, Tokyo, 1988, pp. 185-188

C-1-3

Crystal Defect Study of Solid Phase Epitaxially Grown Si Surrounded by SiO_2 Structures

Eiichi Murakami, Masao Tamura, Kikuo Kusukawa, Masahiro Moniwa, Terunori Warabisako, and Masanobu Miyao

Central Research Laboratory, Hitachi, Ltd.
Kokubunji, Tokyo 185, Japan

Crystal defects in solid phase epitaxially grown Si surrounded by SiO_2 structures are comprehensively studied mainly using a chemical etching technique. The defects are classified into 4 types; dislocations due to surface contamination (type A), microtwins due to {111} facet growth (type B), dislocations due to stress (type C), and defects at facet intersections (type D). Characteristics of type C defects near SiO_2 edge are particularly closely examined. Formation mechanisms of these defects are discussed, on the basis of the experimental results.

1. Introduction

Si solid phase epitaxy (SPE) on Si substrates with patterned SiO_2 films (known as bounded SPE[1]) is a low temperature selective epitaxial growth technique for novel device fabrication.[2] For example, silicon-on-insulator (SOI) structure[3] or sidewall-base-contact structure for bipolar transistor[4,5,2] can be realized using this technique.

Crystal defects in SPE Si have been characterized mainly by transmission electron microscopy (TEM)[6-8]. Microtwins due to {111} facet growth and dislocations are reported. However, detailed characters of these defects have not yet been clarified.

The purpose of the present work is to study these crystal defects comprehensively and to give some insights into their formation mechanisms. Global observation by Nomarski interference optical microscopy with Wright etching is mainly used. The dependence of defect formation on some structural and experimental parameters, i. e. SiO_2 pattern direction, Si thickness, annealing conditions, are investigated.

2. Experiments

Cz-grown {100} oriented Si wafers were utilized as substrates. SiO_2 was thermally grown to a thickness of 25nm for the planar type and 140nm for the LOCOS type. SiO_2 film was patterned into stripes in various directions from <100> to <110>.

Base pressure in the vacuum chamber was about 10^{-8}Pa (Ulta High Vacuum:UHV). The substrate surface was cleaned by Ar beam sputtering and then annealed at 680℃ for 1hr in a UHV. Amorphous Si (a-Si) was deposited at a substrate temperature of 100℃ at 10^{-7}Pa. Typical thickness of the a-Si was 1-4 μm. Deposited a-Si was annealed at 450℃ for 1hr in a UHV for densification and then annealed at 600℃ in a nitrogen atmosphere for SPE. Post SPE annealing (800℃ or 1000℃, 30 min) was performed additionally. The samples were Wright-etched, and then observed by Nomarski interference optical microscopy.

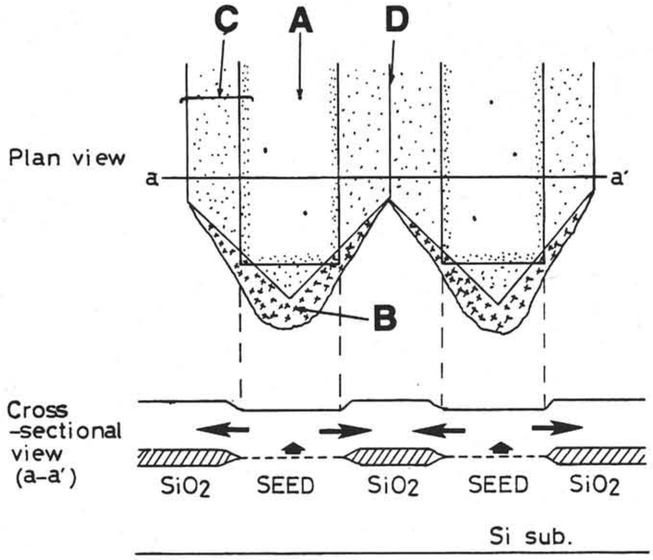

Fig. 1 Classification of crystal defects in SPE Si surrounded by SiO_2 structures

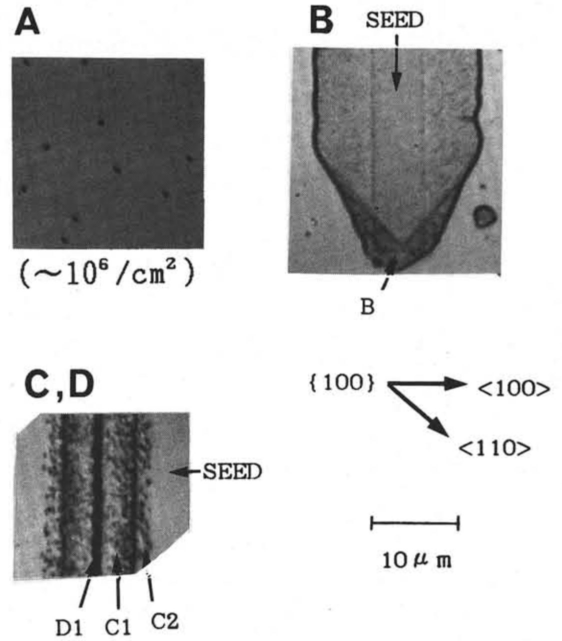

3. Results and Discussion

3.1 Classification of Crystal Defects

Several kinds of defects observed by Nomarski microscope are summarized in Fig. 1. In the on-seed region, type A dislocations are found as etch pits. Etch-pit density is in the order of 10^6 cm^{-2}. Residual contamination (O and C) observed by SIMS must be the origin of these dislocations. In the on-SiO_2 region, microtwins (type B) and dislocations (type C) are observed. Microtwins are found at the corners of convex seeds (Fig. 1 B). This is because {111} facets accompanied by microtwins are preferentially enlarged in these area. Conversely, the {110} facet is dominant and no microtwins are observed in concave seeds.[9]

Type C is classified into C1 and C2, where C1 is observed in the on-SiO_2 region and C2 near the SiO_2 edge in <100> directional SiO_2 patterns.[7] Characteristics of type C2 defect are discussed in detail in the next section.

Type D defects are observed at facet intersections. (Fig. 1 D1). This defect-related phenomena will be discussed in 3. 3.

3.2 Characteristics of dislocations near SiO_2 edges

SiO_2 pattern direction dependence of type C2 defects, dislocations near SiO_2 edges, are shown in Fig. 2. Etch pits are observed in the <110> directional rows starting from the SiO_2 pattern edge. This is most remarkable for the pattern inclined 10° from the <110> pattern ($\theta = 10°$). It is probable that dislocations are on the {111} planes, which are slip planes of Si crystal. Cross sectional representations of samples based on TEM observation[10] are shown in the inset of Fig. 2. Some dislocation lines observed for the <100> pattern start from Si/SiO_2 interface. Dislocations nucleated at the SiO_2/Si interface probably grow and move on {111} planes. The result for the <110> pattern, which shows no dislocation, can be explained by the geometry of the {111} plane and <110> SiO_2 pattern edge; the {111} plane runs parallel to the SiO_2 edge.

The isothermal annealing behavior of the defects is shown in Fig. 3 for <100> and <110> patterns. Between 1 and 2hr annealing time, C2 defects are remarkably multiplied in the <110> pattern. Stress induced by volume change during lateral SPE must be the

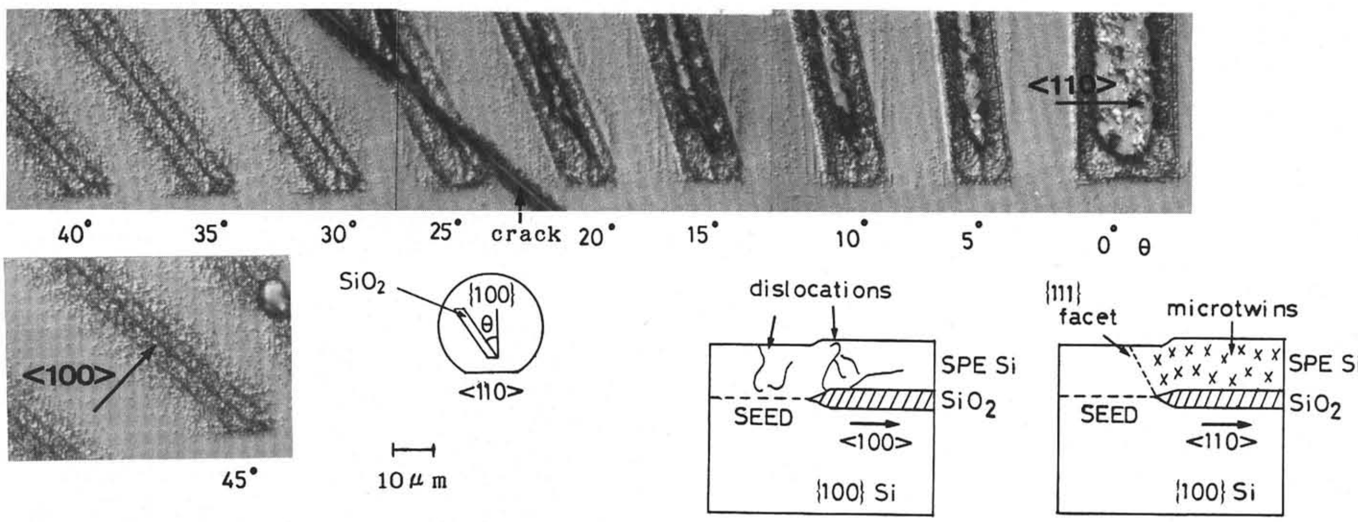

Fig. 2 SiO_2-pattern-direction dependence of type C2 defect formation
(a) Plan view Nomarski micrograph (b) Cross sectional representation based on TEM

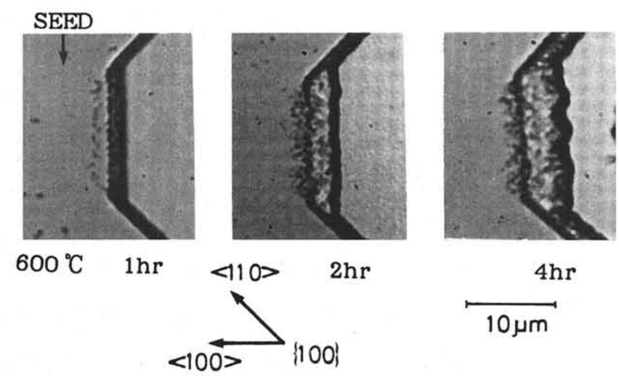

Fig. 3 Multiplication of type C2 defect by isothermal annealing

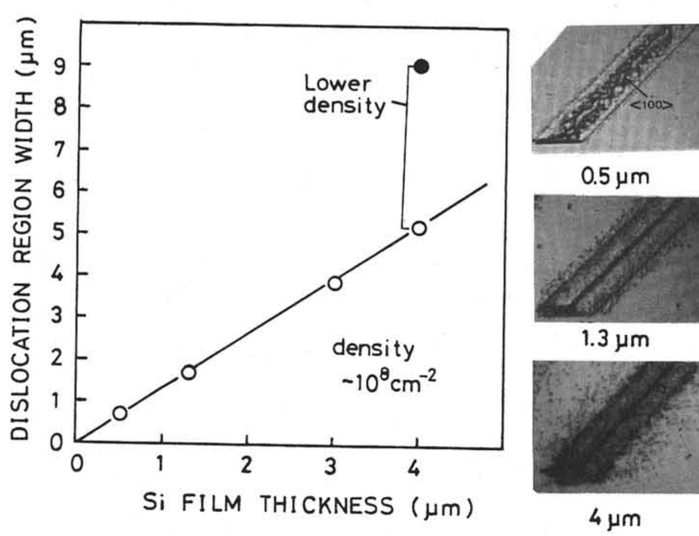

Fig. 4 a-Si film thickness dependence of type C2 defects formation

origin of this defect multiplication.

Amorphous Si film thickness dependence of defect formation is shown in Fig. 4. The dislocation region width (w) is proportional to a-Si thickness (d). This is probably because the extension of the {111} plane from the SiO_2 pattern edge to the surface of on-seed region proportional to d. Anomalous behavior observed in very thick (4μm) film may be due to additional multiplication effects of stronger stress.

3.3 Defects at the intersection of {110} facets

A cross sectional view of D1 defect is illustrated in Fig. 5 (a). This defect is observed at the intersection of two 90° angled {110} facets which form a concave crystal shape. Other combinations of two {110} facets produce similar defects. Type D2, D3 defects are observed at the intersection of 120° angled concave-shaped {110} facets, in on-seed and on-SiO_2 respectively (Fig. 5 (b)). In addition, type D4 defect is observed for 90° angled convex-shaped facets in the on-seed region (Fig. 5 (c))

Annealing behavior of D2, 3, 4 defects are shown in Fig. 6. After 1000℃ 30 min annealing, defects of on-seed region (D3 and especially D4) only appears to be annealed out. Their origin is probably facet mismatch. Thus, the degree of mismatch influences the annealing behavior of type D

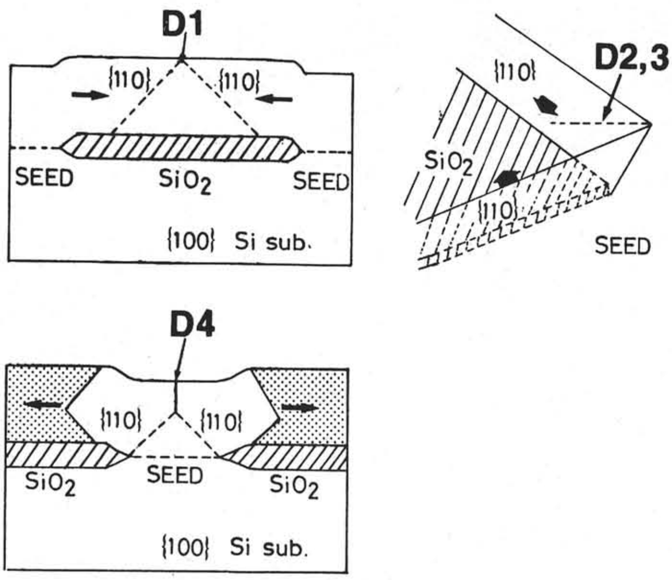

Fig. 5 Illustrations of type D defects
a and c; cross sectional views, b; bird's eye view

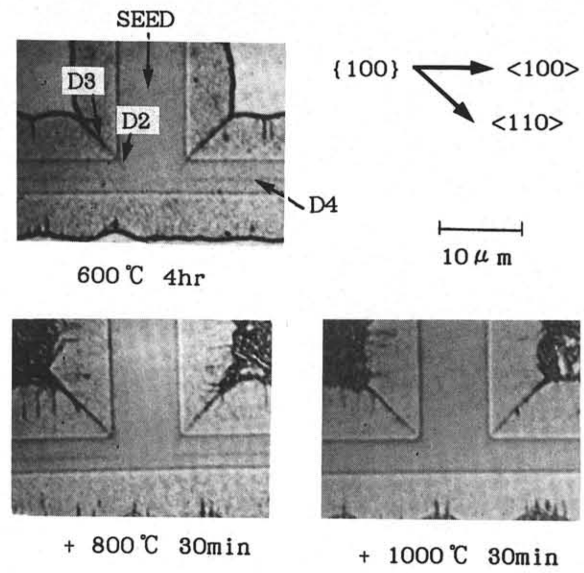

Fig. 6 Annealing behavior of type D2, 3, 4 defects

defects. Detailed observation by TEM is under way.

4. Conclusions

Crystal defects in solid phase epitaxially grown Si surrounded by SiO_2 structures are classified into 4 types; dislocations due to surface contamination (type A), microtwins due to {111} facet growth (type B), dislocations due to stress (type C), and defects at facet intersections. (type D).

Type C defects near the SiO_2 edge appear to nucleate at the Si/SiO_2 interface and grow on {111} planes under stress induced by lateral growth.

Type D defects have several variations depending on the combinations of two {110} facets. The degree of facet mismatch seems to determine the annealing behavior of these defects.

Acknowledgements

The authors are grateful to Drs. Yukio Takano, Yasuo Wada, Eiji Takeda and Mr. Nobuyoshi Natsuaki for their fruitful discussions during the course of this work.

References

1) Y. Kunii, M. Tabe, and K. Kajiyama, J. Appl. Phys. 56 (1984) 279.
2) J. O. Borland, IEDM '87 Tech. Dig. p12.
3) for example, M. Miyao, M. Moniwa, K. Kusukawa, T. Warabisako, E. Murakami, and W. Sinke, Mat. Res. Soc. Symp. Proc. 91 (1987) 387.
4) T. Nakamura, T. Miyazaki, S. Takahashi, T. Kure, T. Okabe, and M. Nagata, IEEE Trans. ED-29 (1982) 596.
5) N. Oh-uchi, A. Kayanuma, K. Asano, H. Hayashi, and M. Noda, IEDM '83 Tech. Dig. p55.
6) M. Tamura, T. Tokuyama, H. Yamamoto, H. Ishiwara, and S. Furukawa, Jpn. J. Appl. Phys. 23 (1984) 1294.
7) Y. Kunii and M. Tabe, Jpn. J. Appl. phys. 24 (1985) L352.
8) H. Kawarada, T. Ueno, Y. Kunii, S. Horiuchi, and I. Ohdomari, Jpn. J. Appl. Phys. 25 (1986) L814.
9) E. Murakami, M. Moniwa, K. Kusukawa, M. Miyao, T. Warabisako, and Y. Wada, J. Appl. Phys. 63 (1988) 4975.
10) K. Kusukawa, M. Moniwa, and M. Tamura, unpublished.